ACS APPLIED MATERIALS & INTERFACES

Research Article

www.acsami.org

Hydrazide Functionalized Core–Shell Magnetic Nanocomposites for Highly Specific Enrichment of *N*-Glycopeptides

Liting Liu,[†,‡,∥,⊥] Meng Yu,[§,⊥] Ying Zhang,[†,‡] Changchun Wang,[*,§] and Haojie Lu[*,†,‡]

[†]Shanghai Cancer Center and Institutes of Biomedical Sciences, Fudan University, Shanghai 200032, P. R. China

[‡]Department of Chemistry, Fudan University, Shanghai 200433, P. R. China

[§]Department of Macromolecular Science, State Key Laboratory of Molecular Engineering of Polymers, Laboratory of Advanced Materials, Fudan University, Shanghai 200433, P. R. China

[∥]Shaanxi Coal and Chemical Technology Institute Co., Ltd., Xi'an 710065, P. R. China

Supporting Information

ABSTRACT: In view of the biological significance of glycosylation for human health, profiling of glycoproteome from complex biological samples is highly inclined toward the discovery of disease biomarkers and clinical diagnosis. Nevertheless, because of the existence of glycopeptides at relatively low abundances compared with nonglycosylated peptides and glycan microheterogeneity, glycopeptides need to be highly selectively enriched from complex biological samples for mass spectrometry analysis. Herein, a new type of hydrazide functionalized core–shell magnetic nanocomposite has been synthesized for highly specific enrichment of *N*-glycopeptides. The nanocomposites with both the magnetic core and the polymer shell hanging high density of hydrazide groups were prepared by first functionalization of the magnetic core with polymethacrylic acid by reflux precipitation polymerization to obtain the Fe_3O_4@poly(methacrylic acid) (Fe_3O_4@PMAA) and then modification of the surface of Fe_3O_4@PMAA with adipic acid dihydrazide (ADH) to obtain Fe_3O_4@poly(methacrylic hydrazide) (Fe_3O_4@PMAH). The abundant hydrazide groups toward highly specific enrichment of glycopeptides and the magnetic core make it suitable for large-scale, high-throughput, and automated sample processing. In addition, the hydrophilic polymer surface can provide low nonspecific adsorption of other peptides. Compared to commercially available hydrazide resin, Fe_3O_4@PMAH improved more than 5 times the signal-to-noise ratio of standard glycopeptides. Finally, this nanocomposite was applied in the profiling of *N*-glycoproteome from the colorectal cancer patient serum. In total, 175 unique glycopeptides and 181 glycosylation sites corresponding to 63 unique glycoproteins were identified in three repeated experiments, with the specificities of the enriched glycopeptides and corresponding glycoproteins of 69.6% and 80.9%, respectively. Because of all these attractive features, we believe that this novel hydrazide functionalized core–shell magnetic nanocomposite will shed new light on the profiling of *N*-glycoproteome from complex biological samples in high throughput.

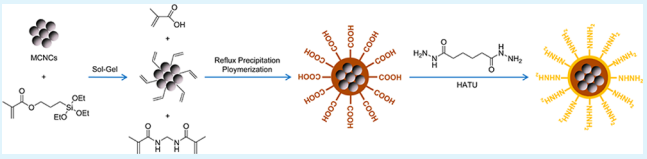

KEYWORDS: *enrichment, glycopeptide, mass spectrometry, nanocomposite, hydrazide chemistry*

1. INTRODUCTION

As one of the most common and complex post-translational modifications (PTMs), the glycosylation of proteins is of extremely great biological significance.[1−3] Glycosylation can affect the three-dimensional structures of proteins or decide the transfer directions of proteins within the cells, and it plays an important role in the recognition between cells and matrixes, signal transduction, and the process of development and differentiation.[4−6] To date, more than half of the discovered cancer biomarkers are glycosylated proteins or peptides;[7] the carbohydrate changes are closely related to the initiation and progression of tumors. Nevertheless, despite more than 50% proteins of the mammalian occur glycosylation, glycopeptides usually exist at relatively low abundance (2−5%) compared with nonglycosylated peptides.[8,9] The glycan microheterogeneity further reduces the relative amount of glycopeptides and decreases the detection sensitivity. In the mass spectrometry (MS) analysis, the signals of glycopeptides are susceptible to the existence of non-glycopeptides; therefore, study of glycosylation is challenging. How to highly and selectively enrich glycopeptides from complex biological samples for MS analysis is a critical problem in glycoproteome research.

Nowadays, diversified techniques for glycopeptide enrichment have sprung up, and these techniques are classified according to different separation mechanisms. Hydrophilic interaction chromatography[10,11] and size exclusion method[12] utilize the difference of physicochemical properties between peptides and glycopeptides; however, high selectivity is hard to achieve. Lectin affinity chromatography (LAC)[13,14] takes the advantage of biospecific recognition between various glycans and different lectins, but LAC has the limitation of capturing only a subset of the glycoproteome associated with the lectin

Received: February 22, 2014
Accepted: April 15, 2014
Published: April 15, 2014

epitope. Hydrazide chemistry,[15,16] boronic acid chemistry,[17−22] and reductive amination[23] methods are based on the chemical bonding between glycopeptides and specific functional groups; therefore, all types of glycopeptides (including N, O, and others types) can be enriched with high specificity. However, boronic acid chemistry can also capture the substances containing cis diols and shows low specificity for complex biological samples. Hydrazide chemistry possesses the highest specificity among these above techniques. This method is widely applied in profiling of *N*-glycoproteome in complex biological samples and extensively combined with stable isotope labeling for the high-throughput identification and quantification of glycosylation sites and glycopeptides.[24−26]

Because of the above mentioned unique advances of hydrazide chemistry, the extensive application of this method contributes to tremendous market demand for hydrazide functionalized materials. To date, many commercial hydrazide functionalized materials are produced by nearly 10 companies. Meanwhile, several new hydrazide functionalized materials with different structures and compositions are also reported.[27−31] Currently, the most commonly used commercial hydrazide functionalized materials are predominantly hydrazide resins and hydrazide functionalized magnetic particles. Nevertheless, hydrazide resins could only be separated from solutions by means of centrifugation, and they are easily partially lost during the process of discarding solutions. For these reasons, the operations using hydrazide resins are time-consuming and incapable of being applied in the large-scale, high-throughput, and automated sample processing. In order to make the hydrazide chemistry method suitable for high-throughput analysis, a magnetic core was introduced into the hydrazide functionalized magnetic particles. Because of the sensitive magnetic response, these materials can be easily separated from solutions with the aid of a magnet. Furthermore, the entire operation is very simple and convenient, which enormously shortened sample processing time. However, hydrazide functionalized magnetic materials are generally prepared through the modification of silane coupling reagents; thus, grafting efficiency and density of hydrazide groups are limited.[27,28] How to smartly combine each unique advantage of hydrazide resins and magnetic nanoparticles to prepare novel magnetic nanomaterials with high density of hydrazide groups is the new developing direction of hydrazide functionalized materials.

Herein, a new type of hydrazide functionalized core−shell magnetic nanocomposites, Fe_3O_4@poly(methacrylic hydrazide) (Fe_3O_4@PMAH), was fabricated by a facile synthesis method. Polymer-coated magnetic nanocomposites with a large number of carboxyl ends were prepared by reflux precipitation polymerization,[32−34] which is a very rapid, simple, and effective method to introduce a large amount of functional groups onto the surface of the magnetic core. After coating with polymer, adipic acid dihydrazide (ADH) was reacted with the surface carboxy to give the hydrazide functionalized polymer magnetic nanocomposites. The abundant hydrazide groups could highly specifically enrich glycopeptides, and the magnetic core makes the nanocomposites easy to be separated from solutions. In addition, the hydrophilic polymer surface can provide low nonspecific adsorption of other peptides. This novel nanocomposite was applied to achieve highly specific glycopeptide enrichment and more convenient profiling of *N*-glycoproteome in real biological samples.

2. EXPERIMENTAL SECTION

Materials. Iron(III) chloride hexahydrate ($FeCl_3·6H_2O$), ammonium acetate (NH_4Ac), ethylene glycol, anhydrous ethanol, trisodium citrate dihydrate, aqueous ammonia solution ($NH_3·H_2O$, 25%), ammonium bicarbonate (NH_4HCO_3), methacrylic acid (MAA), *N*,*N*-dimethylformamide (DMF), 2,2-azobisisobutyronitrile (AIBN), and *O*-(7-azabenzotriazol-1-yl)-*N*,*N*,*N*′,*N*′-tetramethyluronium hexafluorophosphate (HATU) were purchased from Sinopharm Chemical Reagent Co., Ltd (Shanghai, China). *N*,*N*′-Methylenebisacrylamide (MBA), ADH, *N*,*N*-diisopropylethylamine (DIPEA), dithiothreitol (DTT), iodoacetamide (IAA), urea, sodium periodate ($NaIO_4$), α-cyano-4-hydroxycinnamic acid (CHCA), fetuin, asialofetuin, and trypsin were purchased from Sigma-Aldrich (St. Louis, MO). γ-Methacryloxypropyltrimethoxysilane (MPS) was purchased from Jiangsu Chen Guang Silane Coupling Reagent Co., Ltd. Acetonitrile (ACN, analytical reagent (AR)) was purchased from Shanghai Lingfeng Chemical Reagent Company. Acetonitrile (ACN, 99.9%, chromatographic grade), trifluoroacetic acid (TFA), and formic acid (FA) were purchased from Merck (Darmstadt, Germany). Pierce BCA assay kit was purchased from Thermo Scientific (Rockford, IL, USA). The glycerol free peptide-*N*-glycosidase (PNGase F, 500 units/μL) was purchased from New England Biolabs (Ipswich, MA). Sep-Pak C_{18} cartridges were purchased from Waters Associates (Milford, MA, USA). Affi-Gel Hz resin was purchased from Bio-Rad (Hercules, CA, USA). AIBN and MBA were respectively recrystallized from methanol and acetone. DMF and ACN (AR) were both dried and purified via distillation before use. The other reagents were used as received without further purification. Deionized water (18.4 MΩ·cm) used for all experiments was obtained from a Milli-Q system (Millipore, Bedford, MA).

Synthesis of Fe_3O_4@Poly(methacrylic acid) (Fe_3O_4@PMAA) Core−Shell Magnetic Nanocomposites. The Fe_3O_4@PMAA core−shell magnetic nanocomposites were prepared according to our previous work.[33] The magnetite colloidal nanocrystal clusters (MCNCs) were prepared through a modified solvothermal reaction. Typically, $FeCl_3·6H_2O$ (1.350 g), NH_4Ac (3.854 g), and sodium citrate (0.400 g) were dissolved in ethylene glycol (70 mL). The mixture was stirred vigorously for 1 h at 160 °C to form a homogeneous black-red solution and then transferred into a Teflon-lined stainless-steel autoclave (100 mL capacity). The autoclave was heated at 200 °C and maintained for 16.5 h, and then it was cooled to room temperature. The black product was washed with ethanol and collected with the help of a magnet. The cycle of washing and magnetic separation was repeated several times. The final product was dispersed in ethanol for further use.

Modification of MCNCs with MPS was achieved by adding ethanol (40 mL), deionized water (10 mL), $NH_3·H_2O$ (1.5 mL), and MPS (0.3 g) into the MCNCs ethanol suspension and vigorously stirring the mixture for 24 h at 60 °C. The obtained product was separated by using a magnet and washed with ethanol to remove excess MPS. The resultant Fe_3O_4@MPS nanoparticles were dried in a vacuum oven at 40 °C until constant weight was obtained.

Coating the PMAA layer onto Fe_3O_4@MPS nanoparticles was executed by reflux precipitation polymerization of MAA, with MBA as the cross-linker and AIBN as the initiator, in acetonitrile. Typically, Fe_3O_4@MPS seed nanoparticles (25 mg) were dispersed in ACN (20 mL) in a dried single-necked flask (50 mL capacity) with the aid of an ultrasonicator. Then a mixture of MAA (100 mg), MBA (25 mg), and AIBN (2.5 mg) was added to the flask, heated to 90 °C, and kept refluxing for 1 h. Then it was cooled to room temperature. The obtained Fe_3O_4@PMAA nanocomposites were collected by magnetic separation and washed with ethanol to eliminate excess reactants and few generated polymer microspheres.

Synthesis of Fe_3O_4@PMAH Core−Shell Magnetic Nanocomposites. The hydrazide functionalized core−shell magnetic nanocomposites (Fe_3O_4@PMAH) were synthesized with the formation of amide bonds between the carboxyl groups of PMAA and the hydrazide groups of ADH via the amide condensation reaction. Typically, Fe_3O_4@PMAA (50.0 mg) and HATU (132.4 mg) were dissolved in DMF (1.16 mL) at 0 °C in an ice bath with the aid of

ultrasonicator. After the mixture was stirred for 10 min, ADH (55.6 mg) and DIPEA (144 μL) were added into the above DMF solution and was gradually allowed to rise to room temperature. The reaction solution was continuously vortexed for another 3 days at room temperature. The resulting Fe_3O_4@PMAH was washed with DMF, water, and anhydrous ethanol three times in turn for further use.

Analysis of the Hydrazide Density of Fe_3O_4@PMAH. The density of hydrazide groups on Fe_3O_4@PMAH was quantified by BCA assay kit.[35] A standard BCA reagent was obtained by mixing liquid A and liquid B in a ratio of 50:1 (v/v) according to instruction. In a typical procedure, 0−9 μL ADH solutions (0.50 $\mu g \cdot \mu L^{-1}$) were respectively added into 200 μL of standard BCA reagents, and deionized water was added to the total volume of 215 μL. The solutions were afterward gently shaken at 37 °C for 30 min. Meanwhile, three of Fe_3O_4@PMAH (15 μL, 250 μg) respectively reacted with 200 μL of BCA reagent with constant shaking at 37 °C for 30 min. After 215 μL of the mixed ADH and BCA solutions shaking at 37 °C for 30 mins, the absorbance of each mixed ADH and BCA solution was measured at 562 nm using an Infinite 200 (Tecan, Switzerland). According to the relationship between the absorbances of these mixed ADH and BCA solutions and the amounts of hydrazide groups on ADH, a linear calibration curve was obtained. The nanoparticles were separated by a magnet, and then the absorbance of each collected supernatant was also measured at 562 nm. The amount of hydrazide groups on the Fe_3O_4@PMAH was calculated by comparing to the calibration curve.

Characterization. Field-emission transmission electron microscopy (FE-TEM) images were taken on a JEM-2100F transmission electron microscope (JEOL, Japan) at an accelerating voltage of 200 kV. Fourier transform infrared (FT-IR) spectra were performed on a NEXUS-470 FT-IR spectrometer (Nicolet, USA) with potassium bromide pellet. Thermogravimetric analysis (TGA) measurements were performed on a Pyris 1 TGA instrument. All TGA measurements were taken under a constant flow of nitrogen. The temperature was first increased to 100 °C for 5 min and then increased to 800 °C at a rate of 20 $°C \cdot min^{-1}$. Magnetic characterization was carried out with a vibrating sample magnetometer (VSM) on a model 6000 physical property measurement system (Quantum Design, USA) at 300 K. The ζ potential was measured with a ZEN3600 (Malvern, U.K.) Nano ZS instrument using a He−Ne laser at a wavelength of 632.8 nm.

Preparation of Protein Digests. Standard protein (asialofetuin or fetuin) was dissolved in 25 mM NH_4HCO_3 (pH 8.0) and denatured by boiling at 100 °C for 10 min. After cooling to room temperature, trypsin was added to the solution at an enzyme-to-substrate ratio of 1:50 (w/w). The digestion procedure was allowed to proceed at 37 °C overnight, followed by the lyophilization of the digested samples.

Human serum for the experiments was collected from a patient with colorectal cancer with IRB approved protocol from Fudan University Shanghai Cancer Center. An amount of 20 μL of this serum was diluted with the denaturing solution which contained 8 M urea and 0.4 M NH_4HCO_3 (final protein concentration was less than 5 $mg \cdot mL^{-1}$). The mixture was treated with DTT (final concentration was 10 mM) at 60 °C for 60 min and alkylated with IAA (final concentration was 12 mM) at room temperature for 30 min in the dark. Prior to digestion, the solution was diluted with 50 mM NH_4HCO_3 until the final concentration of urea was less than 2 M. Trypsin was added according to the enzyme-to-substrate ratio of 1:50 (w/w) and digested at 37 °C overnight with gentle shaking. The undigested materials were removed by centrifugation at 12000*g* for 10 min. The digests were desalted by C_{18} columns, and the eluted peptides were lyophilized for further use.

Enrichment of *N*-Glycopeptides with Fe_3O_4@PMAH and Hydrazide Resin. The lyophilized sample was redissolved in 50% ACN with 0.1% TFA (0.4 mL), and then oxidized with $NaIO_4$ (10 mM) at room temperature in the dark with constant shaking. After incubation for 1 h, the excess $NaIO_4$ was removed using a Sep-pak C_{18} cartridge and the oxidized peptides were eluted. Pure hydrazide resin (25 μL, 50 μL of 50% slurry) or a certain quality of Fe_3O_4@PMAH was prepared for each sample, and they were prewashed three times with the coupling solution before adding to the above eluted peptide mixture. The oxidized peptide solution was added to hydrazide resin or Fe_3O_4@PMAH, and the glycopeptides were conjugated by mixing at room temperature for 20 h. After coupling of the glycopeptides, the sample was centrifuged or magnetically separated, and then hydrazide resin or Fe_3O_4@PMAH was obtained. Impurities were removed by rinsing the materials three times with each of the following solutions in this order: 500 μL of 80% ACN with 0.1% TFA, 8 M urea with 0.4 M NH_4HCO_3, 100% DMF, and 100 mM NH_4HCO_3. The resin or Fe_3O_4@PMAH was suspended in 100 mM NH_4HCO_3 (100 μL), and PNGase F (1.0 μL) was added and incubated overnight at 37 °C in order to detach the glycans. The supernatant of this procedure was collected and then desalted by C_{18} columns for further analysis.

Mass Spectrometry Analysis. Standard glycopeptides analyses were performed with matrix-assisted laser desorption/ionization time of flight (MALDI-TOF) mass spectrometry. The eluate (1 μL) was deposited on the MALDI plate and air-dried under natural conditions, and then CHCA matrix solution (1 μL) was deposited on the same well of the eluate and air-dried for MS analysis. MALDI-TOF MS analyses were performed in positive reflection mode on a 5800 proteomic analyzer (Applied Biosystems, Framingham, MA, USA) with a Nd:YAG laser at 355 nm, a repetition rate of 400 Hz, and an acceleration voltage of 20 kV. The range of laser energy was optimized to obtain good resolution and signal-to-noise ratio (*S*/*N*) and kept constant for further analysis. The automated acquirement of 5800 MALDI-TOF mass spectra was accomplished through the average of 800 laser shots. External mass calibration was performed by using standard peptides from myoglobin digest. At least three samples were employed in each trial, and three MS runs for each sample were performed in our experiments. The MS data were processed using Data Explorer 4.5 (Applied Biosystems).

1D Nanoflow Liquid Chromatography−Tandem MS (LC−MS/MS) Analysis. Glycopeptides enriched from the digest of human serum were analyzed by 1D nanoflow LC−MS/MS. The deglycosylated and desalted peptide solutions were lyophilized using a vacuum centrifuge and redispersed with 5% ACN containing 0.1% FA (20 μL). The nano-LC−MS/MS experiment was performed on an HPLC system composed of two LC-20AD nanoflow LC pumps, an SIL-20 AC autosampler, and an LC-20AB microflow LC pump (all Shimadzu, Tokyo, Japan) connected to an LTQ-Orbitrap mass spectrometer (Thermo Fisher, San Jose, CA). Sample was loaded onto a CAPTRAP column (0.5 mm × 2 mm, MICHROM Bioresources, Auburn, CA) in 4 min at a flow rate of 20 $\mu L \cdot min^{-1}$. The sample was subsequently separated by a C_{18} reverse-phase column (0.1 mm × 150 mm, packed with 3 μm Magic C_{18}-AQ particles, MICHROM Bioresources, Auburn CA) at a flow rate of 500 $nL \cdot min^{-1}$. The mobile phases were 2% ACN with 0.1% FA (phase A and the loading phase) and 95% ACN with 0.1% FA (phase B). A 90 min linear gradient from 2% to 45% phase B was employed. The separated sample was introduced into the mass spectrometer via an ADVANCE 30 μm silica tip (MICHROM Bioresources, Auburn CA). The spray voltage was set at 1.1 kV and the heated capillary at 200 °C. The mass spectrometer was operated in data-dependent mode, and each cycle of duty consisted of one full-MS survey scan at the mass range 300−1600 Da with resolution power of 100 000 using the Orbitrap section, followed by MS/MS experiments for the 10 strongest peaks using the LTQ section. The AGC expectation during full-MS and MS/MS were 1 000 000 and 10 000, respectively. Peptides were fragmented in the LTQ section using collision-induced dissociation (CID) with helium as the collision gas and the normalized collision energy value set at 35%. Only 2+, 3+, and 4+ peaks were selected for MS/MS runs, and previously fragmented peptides were excluded for 90 s.

Database Search and Data Exploration. The acquired MS/MS spectra were searched against the composite human protein database (combine. human. uniprot. sprot. 090210. fasta 20 331 entries, including both regular and reverse protein sequences)[36] with the SEQUEST algorithm.[37] The search parameters were set as follows: enzyme was selected as trypsin (partially enzymatic). A maximum of two missed cleavages was allowed. Mass value was set as monoisotopic. Carboxamidomethylation (C, +57.021 50 Da) was set as a fixed modification, and the oxidation (M, +15.994 92 Da) and deamidation (N, +0.984 02 Da) were set as variable modifications. Precursor mass

Scheme 1. Synthetic Procedure for Preparation of Fe_3O_4@PMAH Core–Shell Magnetic Nanocomposites

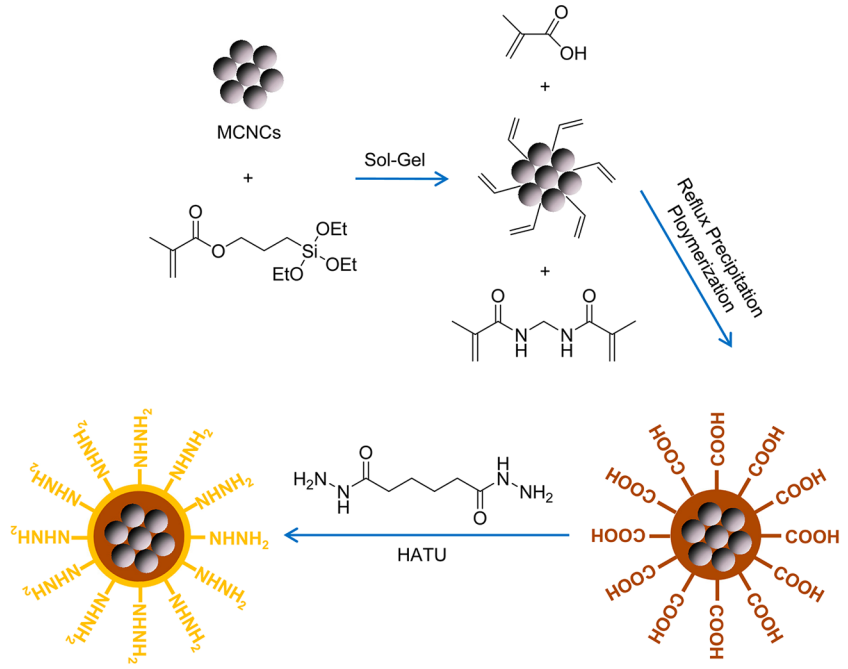

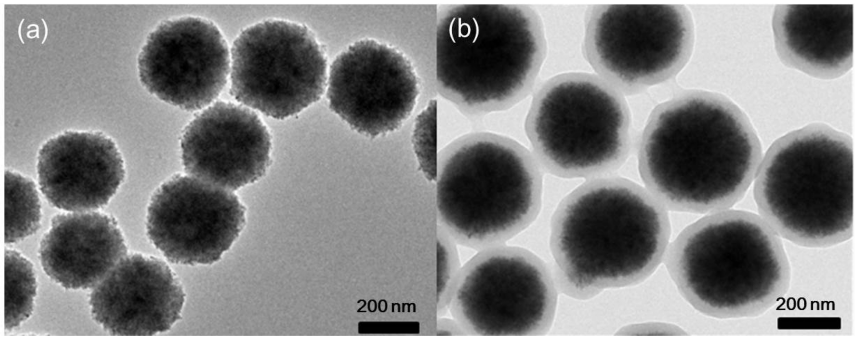

Figure 1. FE-TEM images of (a) MCNCs (Fe_3O_4) and (b) Fe_3O_4@PMAH.

and fragment mass tolerance were 20 ppm and ±1.0 Da for the SEQUEST search. To further validate results obtained from SEQUEST, Trans-Proteomic Pipeline (TPP) was used.[38] Database search results were statistically analyzed using PeptideProphet.[39] By building a well-established nonparametric model using scores and other properties in the search results, PeptideProphet would give high-confidence spectrum-to-peptide interpretation (score of >0.9).[40] Here only those peptides that passed the peptide probability threshold 0.9 and contained the N-X-S/T (X ≠ P) sequences were identified as the glycopeptides.

3. RESULTS AND DISCUSSION

Preparation and Characterization of Fe_3O_4@PMAH. The protocol for synthesis of Fe_3O_4@PMAH core–shell magnetic nanocomposites with high magnetic susceptibility and abundant surface hydrazide groups is schematically illustrated in Scheme 1. First, ~200 nm MCNCs stabilized by citrate were synthesized through a modified solvothermal reaction. Second, the MCNCs were modified with MPS to form active C═C bond on the surface of MCNCs, which was essential for the next step of polymer coating. Third, a robust layer of PMAA was coated on the Fe_3O_4@MPS core by reflux precipitation polymerization of MAA (monomer) and MBA (crosslinker) to form monodisperse magnetic Fe_3O_4@PMAA core–shell nanocomposites. Finally, the hydrazide-functionalized Fe_3O_4@PMAH core–shell magnetic nanocomposites were synthesized with the formation of amide bonds between the abundant carboxyl groups on the Fe_3O_4@PMAA surface and the hydrazine groups of ADH via the amide condensation reaction. Coating functional polymers onto magnetic particles can prepare multifunctional nanocomposites with both the magnetic property of the inner magnetite core and the specific function of the outer polymer shell. For monomers with functional groups such as carboxyl and amino groups, the obtained nanocomposites can be further functionalized. Herein, polymer PMAA with active carboxyl groups was selected to directly coat MCNCs to fabricate nanocomposites with abundant carboxyl groups and good magnetic susceptibility. Before PMAA is coated onto MCNCs, the MCNCs need to be modified with MPS to give vinyl groups on the surface of MCNCs. The active double bond would allow copolymerization among MAA, MBA, and the vinyl groups on the surface of Fe_3O_4@MPS. The polymerization reaction could make the robust PMAA polymer layer coating on the surface of MCNCs and introduce very large amount of carboxyl groups. These ample carboxyl groups provide extremely plentiful reactive sites

for the formation of the amide bond, which highly facilitates the ADH bonding to the surface of Fe_3O_4@PMAA.

The morphology and characteristics of the as-prepared Fe_3O_4@PMAH were measured by the means of various characterization methods. Representative FE-TEM images of MCNCs and Fe_3O_4@PMAA core−shell magnetic nanocomposites are shown in Figure 1. The MCNCs, which consisted of many small nanocrystals, gave an average diameter of ∼200 nm and were uniform in both shape and size. After polymer coating, the surface of Fe_3O_4@PMAA became much smoother than before and the size of the individual particle was obviously enlarged with a narrow size distribution.

FT-IR spectra of the MCNCs, Fe_3O_4@PMAA, and Fe_3O_4@PMAH are compared in Figure 2. The characteristic peaks of

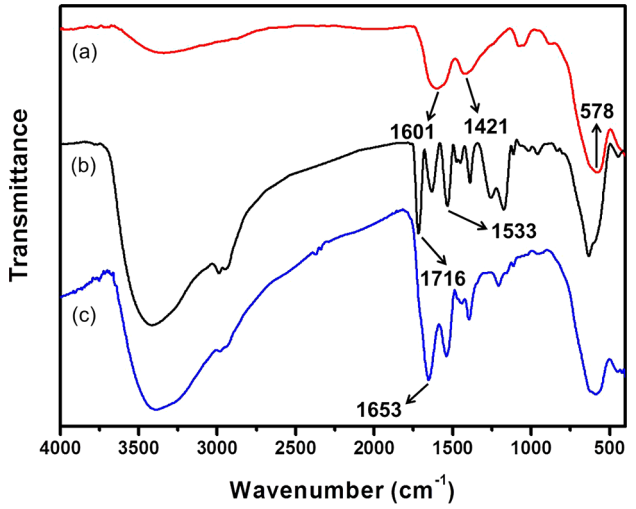

Figure 2. FT-IR spectra of (a) MCNCs (Fe_3O_4), (b) Fe_3O_4@PMAA, and (c) Fe_3O_4@PMAH.

MCNCs are clearly observed at the absorbance of 1601, 1421, and 578 cm^{-1}, and they are attributed to the stretching vibrations of asymmetric COO−, symmetric COO−, and Fe−O, respectively. For Fe_3O_4@PMAA, the new peaks appearing at 1716 and 1533 cm^{-1} attributed to the stretching vibration of C═O of the carboxyl groups and the bending vibration of N−H of MBA demonstrate the successful coating of PMAA onto the surface of MCNCs. As shown in Figure 2c, for Fe_3O_4@PMAH the absorption peak at 1716 cm^{-1} disappeared and a new absorption peak at 1653 cm^{-1} ascribed to the stretching vibration of C═O of ADH proves that most of the carboxyl groups have been modified to the hydrazide groups and that the hydrazide functionalized core−shell magnetic nanocomposites have been obtained.

The composition of Fe_3O_4@PMAH was studied by TGA. The TGA curves of MCNCs, Fe_3O_4@PMAA, Fe_3O_4@PMAH, and pure ADH are shown in Figure 3. The weight loss of MCNCs is about 18 wt %, and this is attributed to the residues of citrate. Fe_3O_4@PMAA also loses its PMAA layer, and the total weight loss is about 67 wt %. Owing to the polymer components in Fe_3O_4@PMAA as well as grafted ADH, the weight loss of Fe_3O_4@PMAH is about 72%. Pure ADH loses almost 97 wt % under the same test condition. The contents of polymer and ADH are calculated to be about 49 and 5 wt %, respectively. Correspondingly, the concentration of grafted ADH was estimated to be 287 $\mu mol \cdot g^{-1}$. The density analysis of hydrazide groups from Fe_3O_4@PMAH was also investigated

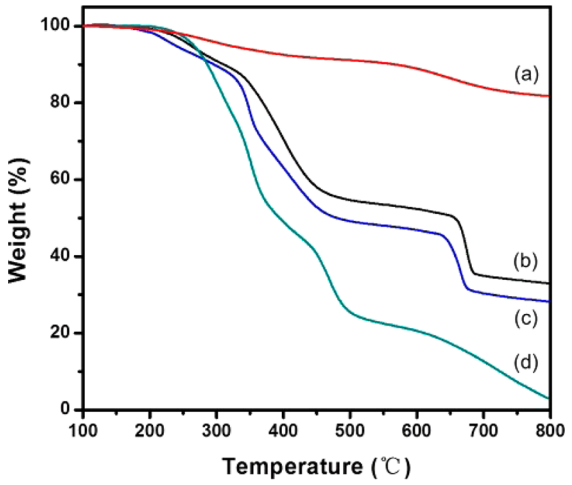

Figure 3. TGA curves of (a) MCNCs (Fe_3O_4), (b) Fe_3O_4@PMAA, (c) Fe_3O_4@PMAH, and (d) pure ADH.

using the BCA method. It can be calculated that the density of hydrazide groups was 154 ± 11 $\mu mol \cdot g^{-1}$, which slightly differed from TGA results. All the above results prove that ADH is successfully grafted to the Fe_3O_4@PMAA and that a high density of hydrazide groups exists on the surface of Fe_3O_4@PMAH.

The ζ potential tests of the materials before and after grafting ADH were also carried out. The ζ potential of Fe_3O_4@PMAA was −40 mV, while after grafting, the ζ potential of Fe_3O_4@PMAH rose to −25 mV. The abundant carboxyl groups on the surface of Fe_3O_4@PMAA provided a large number of negative charges that led to a low negative potential. The potential rose a lot after ADH grafting onto the surface of Fe_3O_4@PMAA. This is because a large portion of carboxyl groups have been grafted with hydrazide groups, which makes the negative charges decrease and consequently the potential rise. Certainly, it is impossible for the grafting efficiency of ADH to achieve 100%; therefore, there are inevitably some existing carboxyl groups that make the overall potential of Fe_3O_4@PMAH negative. The magnetic properties of MCNCs and Fe_3O_4@PMAH were determined by VSM. The magnetic hysteresis curves of MCNCs, Fe_3O_4@PMAA, and Fe_3O_4@PMAH are shown in Figure 4. The saturation magnetization (Ms) value of MCNCs is 73 $emu \cdot g^{-1}$. After encapsulation with a robust layer of PMAA, the saturation magnetization value dramatically decreased to 30 $emu \cdot g^{-1}$ for Fe_3O_4@PMAA. In the end, the saturation magnetization value of Fe_3O_4@PMAH slightly dropped to 28 $emu \cdot g^{-1}$ after grafting of ADH. This result indicates that the effective magnetic content in the nanocomposites is about 38% for Fe_3O_4@PMAH. Although the saturation magnetization value of Fe_3O_4@PMAH decreases greatly compared with the original MCNCs, the magnetic property is still strong enough to ensure that the particles are magnetically separated rapidly. Additionally, no hysteresis curve is observed in Figure 4, which means that all three of these kinds of particles are superparamagnetic at 300 K.

Selective Enrichment of *N*-Glycopeptides with Fe_3O_4@PMAH. The glycopeptide enrichment using Fe_3O_4@PMAH is schematically illustrated in Scheme 2. First, the cis-diol groups on glycans of glycopeptides were converted into aldehydes through the oxidation of sodium periodate. Second, the hydrazone bonds were formed through the reaction between aldehydes and hydrazide groups on Fe_3O_4@PMAH;

dx.doi.org/10.1021/am501110e | ACS Appl. Mater. Interfaces 2014, 6, 7823−7832

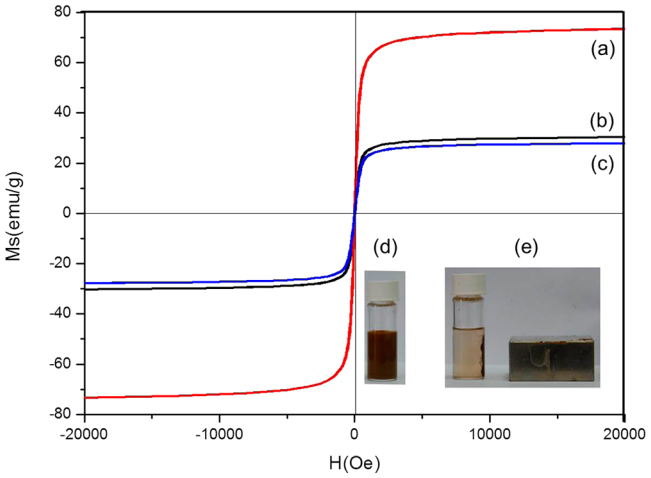

Figure 4. Magnetic hysteresis curves of (a) MCNCs (Fe_3O_4), (b) Fe_3O_4@PMAA, and (c) Fe_3O_4@PMAH; photographs of the Fe_3O_4@PMAH dispersion solution before (d) and after (e) the placement of magnet.

therefore, glycopeptides were captured on the surface of Fe_3O_4@PMAH. Third, four different washing solutions were adopted to rinse the non-glycopeptides adsorbed onto the surface of Fe_3O_4@PMAH. Finally, *N*-glycopeptides were released through deglycosylation by PNGase F.

The performance of Fe_3O_4@PMAH for the selective enrichment of glycopeptides was evaluated by capturing glycopeptides from the digests of two standard glycoproteins fetuin and asialofetuin. MALDI-TOF mass spectra of the fetuin digests before and after enrichment by Fe_3O_4@PMAH are illustrated in Figure 5. Without enrichment, the spectrum is very complex with vast peaks of non-glycopeptides and no signal of glycopeptide was detected (Figure 5a). After enrichment by Fe_3O_4@PMAH, Figure 5b clearly shows that four dominant peaks of the deglycosylated peptides from the standard glycoprotein fetuin digest (asterisks represent the deglycosylated peptides, with *m*/*z* values of 1625.5, 1753.6, 3017.1, and 3556.2) are successfully observed. The *m*/*z* values of 1625.5, 1753.6, 3017.1, and 3556.2 can be attributed to these deglycosylated peptides of LCPDCPLLAPLN#DSR (N# denotes the N-linked glycosylation site); KLCPDCPLLAPLN#DSR; VVHAVEVALATFNAESN#GSYLQLVEISR; RPTGEVYDIEIDTLETTCHVLDPTPLAN#CSVR. These deglycosylated peptides are assigned to the corresponding tryptic glycopeptides of fetuin: LCPDCPLLAPLNDSR + $(GlcNAc)_2(Man)_3(GlcNAc)_2$, KLCPDCPLLAPLNDSR+ $(GlcNAc)_2(Man)_3(GlcNAc)_2$, VVHAVEVALATFNAESNGSYLQLVEISR + $(Glc\ NAc)_2(Man)_3(GlcNAc)_2$, RPTGEVYDIEIDTLETTCHVLDTPLANCSVR + $(Glc\ NAc)_2(Man)_3(GlcNAc)_2$, respectively.

Tryptic digest of the standard glycoprotein asialofetuin was also used to investigate the enrichment efficiency of Fe_3O_4@PMAH for glycopeptides (shown in Figure S1). Before enrichment, the glycopeptides are difficult to be distinguished with only two peaks of glycopeptides from asialofetuin with low intensity because of the presence of large amounts of non-glycopeptides before enrichment (Figure S1a). The peaks observed at *m*/*z* 3740.8 and 5005.6 are assigned to the corresponding tryptic glycopeptides of asialofetuin: RPTGEVYDIEIDTLETTCHVLDPTPLAN#CSVR, and VVHAVEVALATFNAESN#GSYLQLVEISR. After isolation by Fe_3O_4@PMAH, four dominant peaks of the asialofetuin deglycosylated peptides are prominently identified with a clean background. The peaks observed at *m*/*z* 1626.8, 1754.8, 3017.5, and 3558.7 are assigned to these deglycosylated peptides of LCPDCPLLAPLN#DSR, KLCPDCPLLAPLN#DSR, VVHAVEVALATFNAESN#GSYLQLVEISR, and RPTGEVYDIEIDTLETTCHVLDPTPLAN#CSVR. These above results demonstrate that the hydrazide groups successfully grafted on the Fe_3O_4@PMAH can specifically enrich glycopeptides.

Enrichment Capacity of Fe_3O_4@PMAH. Different amounts of Fe_3O_4@PMAH were used to determine the capacity of Fe_3O_4@PMAH to enrich glycopeptides. An amount of 1 mg of the asialofetuin digest was enriched with different

Scheme 2. Overview of the Chemical Reactions Involved in the Enrichment Procedure by Fe_3O_4@PMAH

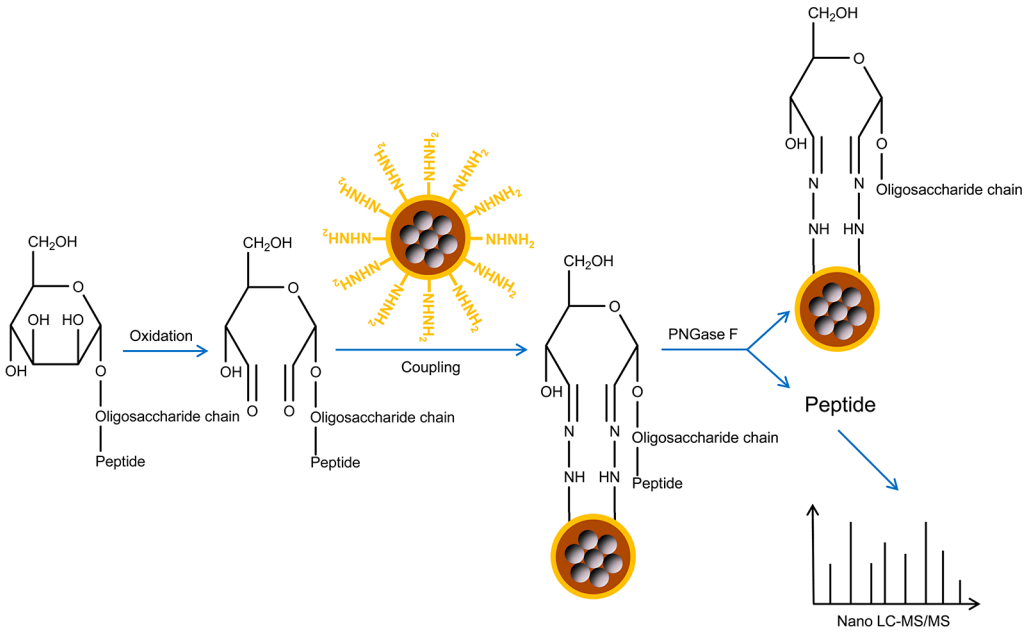

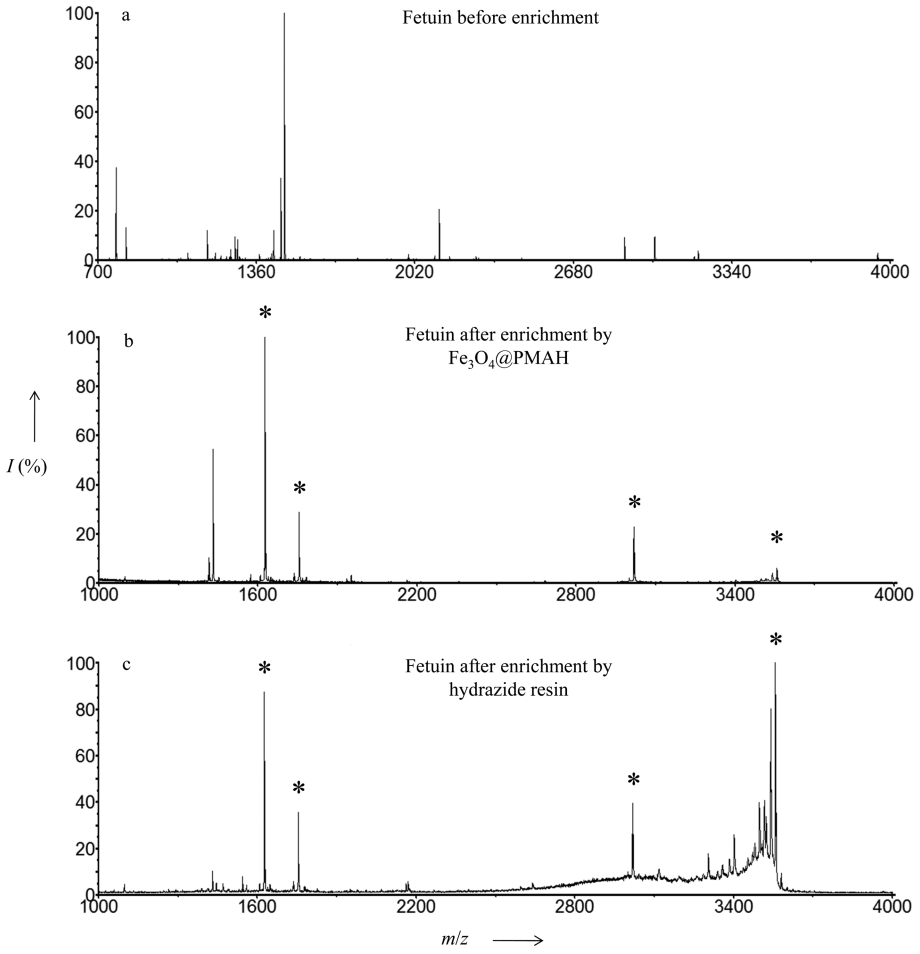

Figure 5. MALDI-TOF mass spectra of the fetuin digests before (a) and after enrichment by Fe_3O_4@PMAH (b) and hydrazide resin (c). The asterisk (∗) denotes the deglycosylated peptides from the fetuin digest, and all peaks in (a) are non-glycopeptides from the fetuin digest.

amounts of Fe_3O_4@PMAH (2, 4, 6, 8, and 10 mg) according to the previous protocol. Each sample solution after glycopeptide enrichment was spotted onto six different wells on a MALDI plate. Then the MS ran three times for each well. Four peaks of glycopeptides were obtained, and the mean values of their absolute intensities were plotted against the addition amounts of Fe_3O_4@PMAH. The influence of addition amounts of Fe_3O_4@PMAH is shown in Figure S2. When the addition amounts of Fe_3O_4@PMAH increased from 2 to 8 mg, the absolute intensities of four peaks of glycopeptides were accordingly increased. The absolute intensities came to the maximum when the amount of Fe_3O_4@PMAH reached 8 mg, afterward the absolute intensities decreased when 10 mg of Fe_3O_4@PMAH was used. The reason for this phenomenon is probably as follows: before the glycopeptide enrichment by Fe_3O_4@PMAH reaches saturation, as the addition amounts of Fe_3O_4@PMAH increase which means the quantity of hydrazide groups increases, the increased amount of captured glycopeptides and higher signal strength of glycopeptides are obtained. Afterward, the glycopeptide enrichment by Fe_3O_4@PMAH reaches saturation. That means the number of hydrazide groups increases to a certain extent which just fully captures all the glycopeptides; hence, the addition amount of material at this point is the optimum dosage. When the addition amount of material is higher than the optimum dosage, the glycopeptide enrichment by Fe_3O_4@PMAH reaches supersaturation. The nonspecific adsorption of deglycosylated peptides on the surface of the material could not be avoided completely. Therefore, the enriching efficiency of Fe_3O_4@PMAH for glycopeptide would be reduced when the addition amount of material was higher than the optimum dosage. For this reason, the optimized addition amounts could be defined as Fe_3O_4@PMAH was added with a ratio of 8 mg of Fe_3O_4@PMAH per 1 mg of protein digests. The enrichment capacity of this method is ∼8 mg of nanocomposites for 1 mg of protein digests, and this excellent enrichment capacity may be due to the high density of hydrazide groups and nanoscale particle size of Fe_3O_4@PMAH.

Comparison of the Enrichment Efficiencies between Fe_3O_4@PMAH and Hydrazide Resin. To further evaluate the enrichment efficiency of Fe_3O_4@PMAH, the same protocol for selective enrichment of glycopeptides from the fetuin digest was employed by both Fe_3O_4@PMAH and the commercialized hydrazide resin. As shown in Figure 5 b,c, four dominant peaks of deglycosylated peptides from the fetuin digest (with m/z values of 1625.5, 1753.6, 3017.1, and 3556.2) are successfully observed with a clean background by both Fe_3O_4@PMAH and hydrazide resin. Compared to hydrazide resin, the S/N of three deglycosylated peptides with m/z values of 1625.5, 1753.6, 3017.1 were respectively improved by 5.8-, 4.6-, and 10.2-fold using Fe_3O_4@PMAH (shown in Table 1). This demonstrates that the enrichment efficiency for glycopeptides by Fe_3O_4@PMAH is superior to that by hydrazide resin. In addition, Fe_3O_4@PMAH could be rapidly separated from solution with a

Table 1. *S/N* of Enriched Deglycosylated Peptides from the Fetuin Digests by Fe_3O_4@PMAH and Hydrazide Resin

	S/N	
m/z	hydrazide resin	Fe_3O_4@PMAH
1625.5	1368	7957
1753.6	572	2614
3017.1	142	1446
3556.2	359	312

magnet because of the design of magnetic core structure, while a tedious centrifuge operation was needed when using hydrazide resin. The protocol of glycopeptide enrichment using Fe_3O_4@PMAH has its own unique advantages superior to those of other hydrazide functionalized materials. The abundant hydrazide groups make it very effective for selective enrichment for glycopeptides from the digest mixture; therefore, the detection signals of glycopeptides could be greatly improved. Furthermore, the entire operation is very simple and convenient, which enormously shortens the sample processing time to 10 s per sample when hydrazide resin needs to be centrifuged for 30 s. In general, this prepared hydrazide functionalized core−shell magnetic nanocomposites combined the advantages of magnetic core, and the high density of hydrazide groups has the potential for application in large-scale, high throughput, and automated sample processing.

***N*-Glycoproteome Profiling of Human Serum by Fe_3O_4@PMAH.** To further evaluate the feasibility of applying the hydrazide functionalized core−shell magnetic nanocomposites for the profiling of glycopeptides from complex biological samples, the profiling of *N*-glycopeptides from the digest of colorectal cancer human serum has been further performed via solid phase extraction with Fe_3O_4@PMAH. The pretreatment process was carried out according to the procedure shown in Scheme 2. An amount of 8 mg of Fe_3O_4@PMAH was used to enrich the *N*-glycopeptides from 20 μL of colorectal cancer human serum digest, and these glycopeptides captured onto the nanocomposites were released through the deglycosylation by PNGase F. In order to verify the reproducibility of this method, three parallel operations for enrichment were performed and three samples of enriched glycopeptides were acquired. Every sample was sent for separation by nano-LC−MS/MS and fragmented by MS/MS using an electrospray ionization linear ion trap quadrupole (ESI-LTQ) Orbitrap instrument. The produced CID spectra were searched against the human protein database. Then the corresponding research results were further statistically analyzed via PeptideProphet software to identify the amino acid sequence as well as N-linked glycosylation sites of glycopeptides. Only those peptides whose confidence scores from PeptideProphet were greater than 0.9 contain the existence of N-X-S/T (X ≠ P) sequences and with the mass increment of 0.984 02 Da of asparagine (N) transforming into aspartic acid (D) could be clearly and definitely affirmed as the *N*-glycopeptides. As shown in Table 2, there is little variance between three experimental data and the quality of identified glycopeptides and their corresponding glycoproteins at each experiment is similar. This indicates that the method of enriching *N*-glycopeptides using Fe_3O_4@PMAH has excellent reproducibility and is feasible for the *N*-glycoproteome profiling of complex biological samples. Among three repeated experiments, the specificities of the enriched glycopeptides are between 66.5% and 69.6%, and the specificities of corresponding glycoproteins are between 78.3% and 80.9%. These results

Table 2. Summary of the Identified Glycopeptides and Glycoproteins from the Digest of Colorectal Cancer Human Serum Using Fe_3O_4@PMAH

identified	enrich 1	enrich 2	enrich 3
unique glycopeptides	135	135	139
unique glycoproteins	55	56	54
unique peptides	194	203	209
unique proteins	68	70	69
glycopeptide specificity	69.6%	66.5%	66.5%
glycoprotein specificity	80.9%	80.0%	78.3%

are a little lower than the previously reported specificities of hydrazide resin for glycopeptides and glycoproteins. This may be attributable to the nonspecific absorption of non-glycopeptides on Fe_3O_4@PMAH caused by the nonspecific interaction between non-glycopeptides and some remanent PMAA on Fe_3O_4@PMAH. The detailed information on identified *N*-glycopeptides and corresponding *N*-glycoproteins from the digest of colorectal cancer human serum using enrichment by Fe_3O_4@PMAH combined with nano-LC−MS/MS analysis is summarized in Table S1 of the Supporting Information. In total, 175 unique glycopeptides and 181 glycosylation sites corresponding to 63 unique glycoproteins are identified in three repeated experiments.

4. CONCLUSIONS

In summary, hydrazide functionalized core−shell magnetic nanocomposites (Fe_3O_4@PMAH) were prepared using the reflux precipitation polymerization and subsequent postgrafting method, as well as applied in the profiling of *N*-glycoproteome from the colorectal cancer patient serum. Fe_3O_4@PMAH possesses the unique advantages of high hydrazide density and magnetic core. On the one hand, the abundant hydrazide groups endow these nanocomposites the excellent enrichment capacity and high specificity for glycopeptides. Compared to hydrazide resin, Fe_3O_4@PMAH improved more than 5 times the signal-to-noise ratio of standard glycopeptides. On the other hand, the magnetic properties of these nanocomposites allow fast separation and ease of operation which results in good reproducibility for the analysis of complex biological samples. For all of the above-mentioned virtues, Fe_3O_4@PMAH, as a kind of novel polymer magnetic nanocomposite, is very promising for the profiling of *N*-glycoproteome from complex biological samples on a large scale and sheds new light upon the discovery of disease biomarkers.

■ ASSOCIATED CONTENT

Ⓢ Supporting Information

More characterization results. This material is available free of charge via the Internet at http://pubs.acs.org.

■ AUTHOR INFORMATION

Corresponding Authors

*C.W.: phone, (+86) 21-55664371; fax, (+86) 21-65640293; e-mail, ccwang@fudan.edu.cn.

*H.L.: phone, (+86) 21-54237618; fax, (+86) 21-54237961; e-mail, luhaojie@fudan.edu.cn.

Author Contributions

⊥L.L. and M.Y. contributed equally to this work.

Notes

The authors declare no competing financial interest.

■ ACKNOWLEDGMENTS

The work was supported by NST (Grants 2012CB910602 and 2012AA020203), NSF (Grants 21025519, 21335002, and 21375026), MOE (Grant 20130071110034), and Shanghai Projects (Eastern Scholar and Grant B109).

■ REFERENCES

(1) Xiong, Z.; Zhao, L.; Wang, F.; Zhu, J.; Qin, H.; Wu, R.; Zhang, W.; Zou, H. Synthesis of Branched PEG Brushes Hybrid Hydrophilic Magnetic Nanoparticles for the Selective Enrichment of N-Linked Glycopeptides. *Chem. Commun.* **2012**, *83*, 8138−8140.

(2) Zhu, J.; Wang, F.; Chen, R.; Cheng, K.; Xu, B.; Guo, Z.; Liang, X.; Ye, M.; Zou, H. Centrifugation Assisted Microreactor Enables Facile Integration of Trypsin Digestion, Hydrophilic Interaction Chromatography Enrichment, and On-Column Deglycosylation for Rapid and Sensitive *N*-Glycoproteome Analysis. *Anal. Chem.* **2012**, *84*, 5146−5153.

(3) Yan, J.; Li, X.; Yu, L.; Jin, Y.; Zhang, X.; Xue, X.; Ke, Y.; Liang, X. Selective Enrichment of Glycopeptides/Phosphopeptides Using Porous Titania Microspheres. *Chem. Commun.* **2010**, *46*, 5488−5490.

(4) Helenius, A.; Aebi, M. Intracellular Functions of N-Linked Glycans. *Science* **2001**, *291*, 2364−2369.

(5) Haltiwanger, R. S.; Lowe, J. B. Role of Glycosylation in Development. *Annu. Rev. Biochem.* **2004**, *73*, 491−537.

(6) Walsh, G.; Jefferis, R. Post-Translational Modifications in the Context of Therapeutic Proteins. *Nat. Biotechnol.* **2006**, *24*, 1241−1252.

(7) Ohtsubo, K.; Marth, J. D. Glycosylation in Cellular Mechanisms of Health and Disease. *Cell* **2006**, *126*, 855−867.

(8) Alvarez-Manilla, G.; Atwood, J.; Guo, Y.; Warren, N. L.; Orlando, R.; Pierce, M. Tools for Glycoproteomic Analysis: Size Exclusion Chromatography Facilitates Identification of Tryptic Glycopeptides with N-Linked Glycosylation Sites. *J. Proteome Res.* **2006**, *5*, 701−708.

(9) Zhang, Y.; Yin, H.; Lu, H. Recent Progress in Quantitative Glycoproteomics. *Glycoconjugate J.* **2012**, *29*, 249−258.

(10) Wuhrer, M.; Koeleman, C. A. M.; Hokke, C. H.; Deelder, A. M. Protein Glycosylation Analyzed by Normal-Phase Nano-Liquid Chromatography−Mass Spectrometry of Glycopeptides. *Anal. Chem.* **2005**, *77*, 886−894.

(11) Ding, W.; Hill, J. J.; Kelly, J. Selective Enrichment of Glycopeptides from Glycoprotein Digests Using Ion-Pairing Normal-Phase Liquid Chromatography. *Anal. Chem.* **2007**, *79*, 8891−8899.

(12) Alvarez-Manilla, G.; Atwood, J., III; Guo, Y.; Warren, N. L.; Orlando, R.; Pierce, M. Tools for Glycoproteomic Analysis: Size Exclusion Chromatography Facilitates Identification of Tryptic Glycopeptides with N-Linked Glycosylation Sites. *J. Proteome Res.* **2006**, *5*, 701−708.

(13) Kaji, H.; Saito, H.; Yamauchi, Y.; Shinkawa, T.; Taoka, M.; Hirabayashi, J.; Kasai, K.; Takahashi, N.; Isobe, T. Lectin Affinity Capture, Isotope-Coded Tagging and Mass Spectrometry to Identify N-Linked Glycoproteins. *Nat. Biotechnol.* **2003**, *21*, 667−672.

(14) Ahn, Y. H.; Kim, Y. S.; Ji, E. S.; Lee, J. Y.; Jung, J. A.; Ko, J. H.; Yoo, J. S. Comparative Quantitation of Aberrant Glycoforms by Lectin-Based Glycoprotein Enrichment Coupled with Multiple-Reaction Monitoring Mass Spectrometry. *Anal. Chem.* **2010**, *82*, 4441−4447.

(15) Zhang, H.; Li, X. J.; Martin, D. B.; Aebersold, R. Identification and Quantification of N-Linked Glycoproteins Using Hydrazide Chemistry, Stable Isotope Labeling and Mass Spectrometry. *Nat. Biotechnol.* **2003**, *21*, 660−666.

(16) Tian, Y.; Zhou, Y.; Elliott, S.; Aebersold, R.; Zhang, H. Solid-Phase Extraction of N-Linked Glycopeptides. *Nat. Protoc.* **2007**, *2*, 334−339.

(17) Liu, L.; Zhang, Y.; Zhang, L.; Yan, G.; Yao, J.; Yang, P.; Lu, H. Highly Specific Revelation of Rat Serum Glycopeptidome by Boronic Acid-Functionalized Mesoporous Silica. *Anal. Chim. Acta* **2012**, *753*, 64−72.

(18) Zhang, L.; Xu, Y.; Yao, H.; Xie, L.; Yao, J.; Lu, H.; Yang, P. Boronic Acid Functionalized Core-Satellite Composite Nanoparticles for Advanced Enrichment of Glycopeptides and Glycoproteins. *Chem.—Eur. J.* **2009**, *15*, 10158−10166.

(19) Qu, Y.; Liu, J.; Yang, K.; Liang, Z.; Zhang, L.; Zhang, Y. Boronic Acid Functionalized Core−Shell Polymer Nanoparticles Prepared by Distillation Precipitation Polymerization for Glycopeptide Enrichment. *Chem.—Eur. J.* **2012**, *18*, 9056−9062.

(20) Ren, L.; Liu, Z.; Liu, Y.; Dou, P.; Chen, H. Ring-Opening Polymerization with Synergistic Co-Monomers: Access to a Boronate-Functionalized Polymeric Monolith for the Specific Capture of *cis*-Diol-Containing Biomolecules under Neutral Conditions. *Angew. Chem., Int. Ed.* **2009**, *48*, 6704−6707.

(21) Li, L.; Lu, Y.; Bie, Z.; Chen, H.; Liu, Z. Photolithographic Boronate Affinity Molecular Imprinting: A General and Facile Approach for Glycoprotein Imprinting. *Angew. Chem., Int. Ed.* **2013**, *52*, 7451−7454.

(22) Zhou, W.; Yao, N.; Yao, G.; Deng, C.; Zhang, X.; Yang, P. Facile Synthesis of Aminophenylboronic Acid-Functionalized Magnetic Nanoparticles for Selective Separation of Glycopeptides and Glycoproteins. *Chem. Commun.* **2008**, *43*, 5577−5579.

(23) Zhang, Y.; Kuang, M.; Zhang, L.; Yang, P.; Lu, H. An Accessible Protocol for Solid-Phase Extraction of N-Linked Glycopeptides through Reductive Amination by Amine-Functionalized Magnetic Nanoparticles. *Anal. Chem.* **2013**, *85*, 5535−5541.

(24) Liu, T.; Qian, W. J.; Gritsenko, M. A.; Camp, D. G., II; Monroe, M. E.; Moore, R. J.; Smith, R. D. Human Plasma *N*-Glycoproteome Analysis by Immunoaffinity Subtraction, Hydrazide Chemistry, and Mass Spectrometry. *J. Proteome Res.* **2005**, *4*, 2070−2080.

(25) Zhang, H.; Liu, A. Y.; Loriaux, P.; Wollscheid, B.; Zhou, Y.; Watts, J. D.; Aebersold, R. Mass Spectrometric Detection of Tissue Proteins in Plasma. *Mol. Cell. Proteomics* **2007**, *6*, 64−71.

(26) Chen, R.; Jiang, X.; Sun, D.; Han, G.; Wang, F.; Ye, M.; Wang, L.; Zou, H. Glycoproteomics Analysis of Human Liver Tissue by Combination of Multiple Enzyme Digestion and Hydrazide Chemistry. *J. Proteome Res.* **2009**, *8*, 651−661.

(27) Zou, Z.; Ibisate, M.; Zhou, Y.; Aebersold, R.; Xia, Y.; Zhang, H. Synthesis and Evaluation of Superparamagnetic Silica Particles for Extraction of Glycopeptides in the Microtiter Plate Format. *Anal. Chem.* **2008**, *80*, 1228−1234.

(28) Sun, S.; Yang, G.; Wang, T.; Wang, Q.; Chen, C.; Li, Z. Isolation of N-Linked Glycopeptides by Hydrazine-Functionalized Magnetic Particles. *Anal. Bioanal. Chem.* **2010**, *396*, 3071−3078.

(29) Tran, T. H.; Park, S. Y.; Lee, H.; Park, S.; Kim, B.; Kim, O. H.; Oh, B.; Lee, D.; Lee, H. Ultrasmall Gold Nanoparticles for Highly Specific Isolation/Enrichment of N-Linked Glycosylated Peptides. *Analyst* **2012**, *137*, 991−998.

(30) Horak, D.; Balonova, L.; Mann, B. F.; Plichta, Z.; Hernychova, L.; Novotny, M. V.; Stulik, J. Use of Magnetic Hydrazide-Modified Polymer Microspheres for Enrichment of *Francisella tularensis* Glycoproteins. *Soft Matter* **2012**, *8*, 2775−2786.

(31) Li, Y.; Zhang, X.; Deng, C. Functionalized Magnetic Nanoparticles for Sample Preparation in Proteomics and Peptidomics Analysis. *Chem. Soc. Rev.* **2013**, *42*, 8517−8539.

(32) Jin, S.; Pan, Y.; Wang, C. Reflux Precipitation Polymerization: A New Technology for Preparation of Monodisperse Polymer Nanohydrogels. *Acta Chim. Sin.* **2013**, *71*, 1500−1504.

(33) Ma, W.; Xu, S.; Li, J.; Guo, J.; Lin, Y.; Wang, C. Hydrophilic Dual-Responsive Magnetite/PMAA Core/Shell Microspheres with High Magnetic Susceptibility and pH Sensitivity via Distillation-Precipitation Polymerization. *J. Polym. Sci., Part A: Polym. Chem.* **2011**, *49*, 2725−2733.

(34) Gao, Q.; Luo, D.; Ding, J.; Feng, Y. Rapid Magnetic Solid-Phase Extraction Based on Magnetite/Silica/Poly(Methacrylic Acid-*co*-Ethylene Glycol Dimethacrylate) Composite Microspheres for the Determination of Sulfonamide in Milk Samples. *J. Chromatogr., A* **2010**, *1217*, 5602−5609.

(35) Smith, P. K.; Krohn, R. I.; Hermanson, G. T.; Mallia, A. K.; Gartner, F. H.; Provenzano, M. D.; Fujimoto, E. K.; Goeke, N. M.;

Olson, B. J.; Klenk, D. C. Measurement of Protein Using Bicinchoninic Acid. *Anal. Biochem.* **1985**, *150*, 76−85.
(36) Moore, R. E.; Young, M. K.; Lee, T. D. Qscore: An Algorithm for Evaluating SEQUEST Database Search Results. *J. Am. Soc. Mass Spectrom.* **2002**, *13*, 378−386.
(37) Havilio, M.; Haddad, Y.; Smilansky, Z. Intensity-Based Statistical Scorer for Tandem Mass Spectrometry. *Anal. Chem.* **2003**, *75*, 435−444.
(38) Nesvizhskii, A. I.; Keller, A.; Kolker, E.; Aebersold, R. A Statistical Model for Identifying Proteins by Tandem Mass Spectrometry. *Anal. Chem.* **2003**, *75*, 4646−4658.
(39) Elias, J. E.; Gygi, S. P. Target-Decoy Search Strategy for Increased Confidence in Large-Scale Protein Identifications by Mass Spectrometry. *Nat. Methods* **2007**, *4*, 207−214.
(40) Malmström, J.; Beck, M.; Schmidt, A.; Lange, V.; Deutsch, E. W.; Aebersold, R. Proteome-Wide Cellular Protein Concentrations of the Human Pathogen *Leptospira interrogans*. *Nature* **2009**, *460*, 762−765.